

Autoregressive Image Generation with Linear Complexity: A Spatial-Aware Decay Perspective

Yuxin Mao¹ Zhen Qin² Jinxing Zhou⁴ Hui Deng¹
Xuyang Shen³ Bin Fan¹ Jing Zhang⁵ Yiran Zhong³ Yuchao Dai^{1†}
¹Northwestern Polytechnical University ²TapTap ³OpenNLPLab
⁴Hefei University of Technology ⁵Australian National University

Abstract

*Autoregressive (AR) models have garnered significant attention in image generation for their ability to effectively capture both local and global structures within visual data. However, prevalent AR models predominantly rely on the transformer architectures, which are beset by quadratic computational complexity concerning input sequence length and substantial memory overhead due to the necessity of maintaining key-value caches. Although linear attention mechanisms have successfully reduced this burden in language models, our initial experiments reveal that they significantly degrade image generation quality because of their inability to capture critical long-range dependencies in visual data. We propose Linear Attention with Spatial-Aware Decay (LASAD), a novel attention mechanism that explicitly preserves genuine **2D spatial relationships within the flattened image sequences** by computing position-dependent decay factors based on true 2D spatial location rather than 1D sequence positions. Based on this mechanism, we present LASADGen, an autoregressive image generator that enables selective attention to relevant spatial contexts with linear complexity. Experiments on ImageNet show LASADGen achieves state-of-the-art image generation performance and computational efficiency, bridging the gap between linear attention’s efficiency and spatial understanding needed for high-quality generation.*

1. Introduction

Recent advances in deep generative modeling [1–7] have led to significant progress in the field of image generation. Traditionally, image generation has been dominated by GAN-based models [8–10] or diffusion models [11], which produce high-quality images through adversarial training or iterative denoising processes. However, the recent success of large-scale language models (LLM) [12–14] spark a resurgence of interest in autoregressive methods for vi-

sual generation. These methods, which are inspired by the architectures of language modeling, treat images as sequences of visual tokens (either pixels or patches), enabling the simultaneous modeling of both local contextual relationships and global compositional structures. This shift not only achieves competitive image generation performance but also opens up exciting possibilities for unifying the modeling of visual and linguistic modalities.

However, traditional autoregressive image generation models usually employ the Transformer [15] architecture to process image sequences. As the sequence length of the image tokens N increases, the model exhibits quadratic $O(N^2)$ complexity, and a large number of Key-Value pairs need to be stored and updated as the sequence length increases. This memory-intensive process leads to a significant computational burden, especially for high-resolution images. In contrast, linear attention [16, 17] or hybrid models with approximate linear complexity [18, 19] has been extensively explored and successfully applied in large language models, offering a more efficient solution with linear complexity. This adaptation dramatically reduces the memory overhead while maintaining the ability to model dependencies across the input sequence. Therefore, this raises an important question: *Can linear attention be effectively applied to autoregressive image generation models without compromising performance?*

In response to this question, we conduct a series of explorations. We replace the standard multi-head self-attention (SoftmaxAttn) layers in our baseline autoregressive image generator with ordinary linear attention (see Tab. 2) and find significantly degraded generation quality compared with the SoftmaxAttn-based model. Analysis reveals this poor performance stems from linear attention’s inability in capturing global context [20, 21], limiting its ability in modeling long-range dependencies. To address this limitation, we further explore the advanced linear attention methods from natural language processing that employ weighted decay [22–26] of relative positions or attention weights to enhance local context modeling (see Tab. 2).

However, despite implementing the decay mechanism, our experimental results show that the image generation quality remains suboptimal.

This performance degradation reveals that the conventional decay mechanisms designed for language models fail in image generation precisely because of their inability to handle the fundamental dimensional mismatch when 2D spatial data are flattened into 1D sequences. To overcome this limitation, we propose Linear Attention with Spatial-Aware Decay (LASAD), a novel approach that addresses the limitations of decay-based linear attention in image generation. Our method incorporates a Spatial-Aware Decay (SAD) strategy that explicitly accounts for the 2D nature of images when applying the attention mechanisms. LASAD works by computing position-dependent decay factors that preserve 2D spatial relationships in the raster scan flattened image sequence, enabling the model to differentiate between image patches that are spatially adjacent versus those that are merely adjacent in the flattened representation.

We implement the Spatial-Aware Decay strategy through a simple location-based decay function, which requires only *a few lines of code*, yet effectively modulates the decay factor according to true spatial locations rather than the sequence positions. Furthermore, our architecture integrates these LASAD layers throughout the generator network (resulting in LASADGen), replacing conventional attention mechanisms in the LlamaGen framework [6] while maintaining autoregressive generation capabilities. Extensive experiments on ImageNet dataset [27] demonstrate that LASADGen achieves state-of-the-art performance in terms of computational efficiency and image generation quality.

Our contributions can be summarized as follows:

- We propose LASAD, a novel linear attention mechanism with spatial-aware decay that preserves 2D relationships in flattened image sequences while maintaining linear computational complexity.
- We conduct comprehensive analyses on why standard linear attention and attention decay variants fail in autoregressive image generation, identifying the critical importance of preserving spatial context in visual data.
- We develop LASADGen, which integrates our LASAD layers to achieve state-of-the-art performance with significantly reduced computational cost compared with the transformer-based approaches.

2. Related Works

Autoregressive Visual Generation Methods. Visual generation has gained significant attention in recent years, particularly with the advancement of deep learning architectures and generative models [3–6]. A key trend is the use of autoregressive models [12, 13], which exhibit substantial generality and potential, owing to their strong connection with natural language processing (NLP). Autoregressive

generation methods are typically categorized into two main approaches: BERT-style masked autoregressive models and GPT-style autoregressive models. Masked autoregressive methods [28–31], inspired by BERT-style pretraining [32], generate images by predicting randomly masked tokens. In contrast, GPT-style autoregressive models [13, 33, 34] employ image tokenization techniques [35, 36] to convert images into discrete representations, enabling sequential next-token prediction. Recently, LlamaGen [6] extends autoregressive methods by adapting Llama [12] and similar large language model architectures for image token prediction. By applying the “next-token prediction” paradigm to visual generation, LlamaGen demonstrates competitive performance in image generation tasks. Meanwhile, VAR [37] adjusts the paradigm of autoregressive generation and design “next-scale prediction”, which is also a successful application of autoregression in visual generation tasks. Due to the scalability of LlamaGen, there are still many works expanding on it, such as visual token decoding methods [38–40], stronger visual tokenizers [41], more effective model structures [42, 43], *etc.*

Linear Attention. Linearized attention challenges the traditional quadratic complexity of softmax attention by utilizing kernel-based methods to decompose attention computations. Rather than computing the full attention matrix, linear attention projects queries and keys into a transformed space, where the interactions can be computed with linear complexity $O(N)$ relative to the sequence length. The evolution of linear attention has followed several innovative trajectories. Katharopoulos *et al.* [20] posits that positive kernel functions, such as $\text{elu}(x) + 1$, can be used to approximate nonlinear **softmax** function. Consequently, this enables linearization of attention while maintaining numerical stability. This insight paved the way for a new family of attention variants. The Random Feature Attention (RFA) framework [44] introduced probabilistic approximations using random Fourier features, while Performer [45] advanced this concept by designing positive random features that better preserve the exponential characteristics of softmax attention. Cosformer [21] decomposes attention based on trigonometric principles, achieving linear complexity while preserving crucial theoretical properties of softmax attention. Recent advances in linear attention mechanisms frequently incorporate decay functions to enhance token locality, as demonstrated in models such as TNL [17], GLA [22], RetNet [23], and HGRN [24, 25], *etc.* This decay approach effectively addresses the uniform weighting limitation inherent in traditional linear attention by exponentially discounting contributions from older tokens, preventing attention saturation issues.

Uniqueness of Our Solutions. Although linear attention has been fully explored and applied in many fields, our approach transcends the naive application of linear attention

mechanisms to autoregressive image generation by addressing a fundamental limitation: the dimensional mismatch that occurs when 2D image data is flattened into 1D sequences. This flattening disrupts the spatial relationships between image patches that are crucial for coherent image generation. Therefore, while linear attention mechanisms offer computational efficiency benefits, we need to explore how spatial context is preserved in visual data.

3. Method

Our approach is based on the autoregressive model. Particularly, we identify the performance degradation issues arising from applying decay-based linear attention to flattened 2D images and aim to solve the problems of preserving authentic spatial relationships while maintaining computational efficiency in autoregressive image generation. In this section, we first define the basic paradigm of visual autoregressive generation (Sec. 3.1), then explore visual autoregressive generation with linear complexity (Sec. 3.2 and Sec. 3.3), and finally propose a simple yet effective Spatial-Aware Decay mechanism (Sec. 3.4). The complete algorithm is shown in Algorithm 1.

3.1. Autoregressive Visual Generation

In autoregressive visual generation, an image $I \in \mathbb{R}^{H \times W \times 3}$ is first quantized into a discrete token map $X \in \mathbb{R}^{h \times w}$ by an image tokenizer, where $h = H/p$ and $w = W/p$ with p being the down-sampling rate of the tokenizer. Following raster scanning order, X is reshaped into a 1D sequence (x_1, x_2, \dots, x_N) where $N = h \times w$ represents the total number of image tokens.

Autoregressive models define the generative process as sequential next-token prediction:

$$p(\mathbf{x}) = \prod_{t=1}^N p(x_t | x_1, x_2, \dots, x_{t-1}) = \prod_{t=1}^N p(x_t | x_{<t}), \quad (1)$$

where x_t denotes the discrete image token at position t . Contemporary autoregressive image generation models, such as LlamaGen [6], typically incorporate conditioning information c (e.g., class labels or text embeddings) into the generation process:

$$p(\mathbf{x}|c) = \prod_{t=1}^N p(x_t | x_{<t}, c). \quad (2)$$

To model these sequences, a causal Transformer architecture is commonly employed, trained by minimizing the next-token prediction loss:

$$\mathcal{L}_{\text{train}} = \text{CE}(\mathbf{M}([c, x_1, x_2, \dots, x_{t-1}]), [x_1, x_2, \dots, x_t]), \quad (3)$$

Algorithm 1 Algorithm of the proposed Linear Attention with Spatial-Aware Decay (Sequential version).

```

1: Input: Input sequence  $\mathbf{X} \in \mathbb{R}^{B \times N \times D}$ , image width  $w$ 
   (in tokens)
2: Output: Output sequence  $\mathbf{O} \in \mathbb{R}^{B \times N \times D}$ 
3:  $\mathbf{s}_0 \leftarrow \mathbf{0}$ 
4: for  $t = 1$  to  $N$  do
5:    $\mathbf{v}_t, \mathbf{q}_t, \lambda_t \leftarrow \text{Linear}(\mathbf{x}_t)$ 
6:    $\mathbf{q}_t \leftarrow \text{Silu}(\mathbf{q}_t)$ 
7:    $\lambda_t \leftarrow \text{Sigmoid}(\lambda_t)$ 
8:    $\mathbf{k}_t \leftarrow 1 - \lambda_t$ 
9:    $\lambda_t^{\text{spatial}} \leftarrow \mathbf{f}_t$ 
10:  if  $(t \bmod w) = 0$  then
11:     $\lambda_t^{\text{spatial}} \leftarrow 1$  ▷ Set decay factor to 1 at row boundaries
12:  end if
13:   $\mathbf{s}_t \leftarrow \text{diag}(\lambda_t^{\text{spatial}}) \mathbf{s}_{t-1} + \mathbf{k}_t \cdot \mathbf{v}_t^\top$ 
14:   $\mathbf{o}_t^\top \leftarrow \mathbf{q}_t^\top \cdot \mathbf{k} \mathbf{v}_t$ 
15:   $\mathbf{o}_t \leftarrow \text{Linear}(\text{Norm}(\mathbf{o}_t))$ 
16: end for
17: return  $\mathbf{O} = [\mathbf{o}_1, \mathbf{o}_2, \dots, \mathbf{o}_n]$ 

```

where CE denotes the cross-entropy loss and \mathbf{M} represents the generative model, typically implemented as a Transformer architecture [15].

While this approach shows promise in image generation [6], it faces substantial computational challenges. Traditional Transformer attention has quadratic $O(N^2)$ complexity as each token attends to all others. This computational bottleneck motivates us to explore more efficient attention mechanisms that maintain generation quality.

3.2. Linear Attention for Computational Efficiency

Standard attention computes outputs as weighted sums of values, with weights determined by query-key interactions followed by softmax normalization [15]:

$$\text{Attention}(\mathbf{Q}, \mathbf{K}, \mathbf{V}) = \text{softmax}\left(\frac{\mathbf{Q}\mathbf{K}^\top}{\sqrt{d_k}}\right) \mathbf{V}, \quad (4)$$

where $\mathbf{Q}, \mathbf{K}, \mathbf{V} \in \mathbb{R}^{N \times d}$ represent the query, key, and value matrices, respectively, N is the number of tokens in the input sequence, d is the dimension of the token embeddings. This formulation incurs $O(N^2)$ complexity, becoming computationally prohibitive for long sequences.

Linear attention addresses this limitation by replacing the softmax with a kernel function $\phi(\cdot)$ [20, 21, 45], allowing for a reformulation:

$$\mathbf{O} = \Delta^{-1} \phi(\mathbf{Q}) [\phi(\mathbf{K})^\top \mathbf{V}], \quad \Delta = \text{diag}(\phi(\mathbf{Q}) [\phi(\mathbf{K})^\top \mathbf{1}_N]). \quad (5)$$

By computing $\phi(\mathbf{K})^\top \mathbf{V}$ first, the time complexity is reduced to $O(N)$. [46] observed that the denominator Δ can

destabilize training and proposed to replace it with normalization functions:

$$\mathbf{O} = \text{Norm}(\phi(\mathbf{Q})[\phi(\mathbf{K})^\top \mathbf{V}]). \quad (6)$$

In causal autoregressive settings, linear attention can be expressed recursively (omitting normalization and kernel function for clarity) [20]:

$$\begin{aligned} \mathbf{s}_0 = \mathbf{0}, \mathbf{s}_t = \mathbf{s}_{t-1} + \mathbf{k}_t \mathbf{v}_t^\top, \mathbf{o}_t^\top = \mathbf{q}_t^\top \mathbf{s}_t, \\ \mathbf{q}_t, \mathbf{k}_t, \mathbf{v}_t, \mathbf{o}_t \in \mathbb{R}^d, \mathbf{s}_t \in \mathbb{R}^{d \times d}, \\ t = 1, \dots, N. \end{aligned} \quad (7)$$

The above formulation significantly reduces the computational complexity. However, our initial attempts reveal that directly replacing standard attention with linear attention in autoregressive image generation models leads to performance degradation (see Tab. 2). This observation motivates us to investigate strategies to enhance the effectiveness of linear attention in an autoregressive framework.

3.3. Linear Attention with Decay Mechanisms

Recent advances in language modeling demonstrate that incorporating decay mechanisms into linear attention significantly improves modeling of long-range sequential dependencies [24, 25, 47]. This decay approach mitigates the uniform weighting problem of traditional linear attention by exponentially discounting older token contributions, allowing the model to prioritize more recent and relevant information while preventing attention saturation over long sequences [48]. Specifically, linear attention with decay introduces a decay factor λ_t into the recursive formulation:

$$\begin{aligned} \mathbf{s}_0 = \mathbf{0}, \mathbf{s}_t = \text{diag}(\lambda_t) \mathbf{s}_{t-1} + \mathbf{k}_t \mathbf{v}_t^\top, \mathbf{o}_t^\top = \mathbf{q}_t^\top \mathbf{s}_t, \\ \mathbf{q}_t, \mathbf{k}_t, \mathbf{v}_t, \mathbf{o}_t, \lambda_t \in \mathbb{R}^d, \mathbf{s}_t \in \mathbb{R}^{d \times d}, \\ 0 \leq \lambda_t \leq 1, t = 1, \dots, N. \end{aligned} \quad (8)$$

The decay parameter λ_t controls the retention of historical information. A constant $\lambda_t = \lambda$ represents data-independent decay [23, 47], which offers computational efficiency but lacks adaptability to varying content importance, while input-dependent λ_t constitutes data-dependent decay [22, 24, 25, 49], providing more flexible information retention that can prioritize contextually relevant tokens at the cost of increased computational complexity. Both approaches present distinct trade-offs in the context-length versus computation spectrum.

One advanced implementation of this approach is HGRN2 [25], which associates the input gate in linear RNN with the key in linear attention, the output gate with the query, and the input with the value. It uses a parameter-sharing strategy for the decay and the input gate/key, and

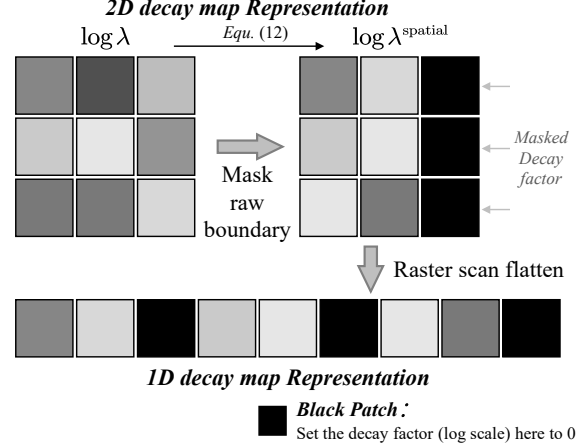


Figure 1. **Visualization of the Spatial-Aware Decay mechanism.** Each color block represents the decay factor of the token at the corresponding position. Our method applies a mask (black in the figure) at row boundaries when raster scan flattening, preventing inappropriate information flow between non-adjacent image tokens.

utilizes an outer product for expansion:

$$\begin{aligned} \mathbf{s}_0 = \mathbf{0}, \mathbf{s}_t = \text{diag}(\lambda_t) \mathbf{s}_{t-1} + (1 - \lambda_t) \mathbf{v}_t^\top, \mathbf{o}_t^\top = \mathbf{q}_t^\top \mathbf{s}_t, \\ \mathbf{q}_t, \mathbf{v}_t, \mathbf{o}_t, \lambda_t \in \mathbb{R}^d, \mathbf{s}_t \in \mathbb{R}^{d \times d}, \\ 0 \leq \lambda_t \leq 1, t = 1, \dots, N. \end{aligned} \quad (9)$$

Despite their success in language modeling, our experiments (see Tab. 4) reveal that direct application of decay mechanisms to image generation yields suboptimal results. The fundamental challenge stems from flattening 2D image data into 1D sequences. Unlike text data, which is naturally sequential, this raster-scan based flatten method distorts the spatial relationships in images, causing tokens from disparate spatial regions to become adjacent in the sequence representation. Consequently, the decay mechanism fails to accurately model the true spatial relationships in the original 2D structure, thus the model may misinterpret distant regions as neighboring ones.

3.4. Spatial-Aware Decay Mechanism

To address the challenges of preserving spatial relationships in flattened 2D image data, we propose a simple yet effective mechanism termed Spatial-Aware Decay (SAD). SAD extends the HGRN2 by making the gating mechanism spatially aware, specifically targeting the problem of row transitions in flattened 2D data. Building on the recursive formulation from Eq. (9), our SAD mechanism is defined as:

$$\begin{aligned} \mathbf{s}_0 = \mathbf{0}, \mathbf{s}_t = \text{diag}(\lambda_t^{\text{spatial}}) \mathbf{s}_{t-1} + \mathbf{k}_t \mathbf{v}_t^\top, \mathbf{o}_t^\top = \mathbf{q}_t^\top \mathbf{s}_t, \\ \mathbf{q}_t, \mathbf{k}_t, \mathbf{v}_t, \mathbf{o}_t, \lambda_t^{\text{spatial}} \in \mathbb{R}^d, \mathbf{s}_t \in \mathbb{R}^{d \times d}, \\ 0 \leq \lambda_t \leq 1, t = 1, \dots, N, \end{aligned} \quad (10)$$

Table 1. **Details of LASAD models.** We follow the configurations of LlamaGen [6] and get different variants.

Model	Layers L	Hidden size d	Heads	#Para.
LASAD-B	12	768	12	111M
LASAD-L	24	1024	16	346M
LASAD-XL	36	1280	20	774M
LASAD-XXL	48	1536	24	1.4B

where $\lambda_t^{\text{spatial}}$ is our proposed spatially-aware decay factor. We compute this factor by first deriving a base decay factor from the key vector:

$$\lambda_t = 1 - \mathbf{k}_t. \quad (11)$$

We then modify this base decay factor at specific intervals that correspond to row transitions in the original 2D image. Our key motivation is to preserve the authentic spatial relationship of the original 2D image by setting decay values to one between non-adjacent tokens at row boundaries, thereby preventing inappropriate information propagation across spatially disconnected regions when flattening the image tokens. Fig. 1 illustrates how our Spatial-Aware Decay mechanism handles the transition from 2D to 1D representation by resetting decay factors at row boundaries, maintaining the authentic spatial relationships when processing flattened image tokens. Thus, the spatially-aware decay factor $\lambda_t^{\text{spatial}}$ is computed as:

$$\log \lambda_t^{\text{spatial}} = \log \lambda_t \cdot \mathbb{I}(t \bmod w), t = 1, \dots, N, \quad (12)$$

where \bmod denotes the modulo operation, t is the position of the token in the flattened 1D sequence, w is the width of the image tokens, and $\mathbb{I}(\cdot)$ is the indicator function that outputs 1 when the argument is true and 0 otherwise. This formulation captures row transitions at positions where t is the last token in a row.

Our modification sets log decay factors to zero at row boundaries in the flattened sequence, effectively resetting accumulated state between rows. This prevents inappropriate influence between tokens that are not spatially adjacent in the original 2D image layout. By enforcing this reset at row transitions, the model respects the inherent 2D structure of images, allowing linear attention to better capture both local details and global composition. Unlike standard uniform decay mechanisms, our Spatial-Aware Decay specifically addresses distortions introduced when flattening 2D data. This approach aligns attention mechanisms with true spatial relationships in the image, balancing the preservation of important cross-row dependencies while preventing spurious connections between distant regions. The result is improved image generation quality while maintaining the computational efficiency of linear attention.

4. Experiments

4.1. Implementation Details

Benchmark. We develop LASADGen by extending the LlamaGen architecture [6], since it is a simple and scalable framework for autoregressive image generation. For comprehensive evaluation, we conduct experiments on class-conditional image generation using the ImageNet1K [27], which serves as a standard benchmark in the field.

Evaluation Metrics. We evaluate our method using the Fréchet Inception Distance (FID) [50] as the primary metric, complemented by the Inception Score (IS) [51] and precision-recall metrics [52]. For fair comparison, we directly cite baseline results from their respective original papers. All quantitative evaluations are conducted using the official TensorFlow implementation from ADM [53] to ensure consistent measurement conditions.

Training Details. We conduct our experiments trained on ImageNet1K [27] at 256×256 resolution. The training is performed on 8 NVIDIA H800 GPUs (80GB), with each image being discretized into 256 tokens. For optimization, we employ AdamW with momentum parameters $(\beta_1, \beta_2) = (0.9, 0.95)$ and a weight decay coefficient of 0.05. The learning rate is set to 1×10^{-4} for a batch size of 256, and the models are trained for 300 epochs. To enable classifier-free guidance [54] during inference, we applied a dropout rate of 0.1 to the class embedding layers. The image tokenizer incorporates a downsampling factor of 16 and leverages pre-trained weights from LlamaGen [6]. We use the Flash Linear Attention library [55] to get an efficient linear attention implementation.

4.2. Model Configurations

The proposed LASADGen model consists of L LASAD blocks, each with the hidden dimension size d . Consistent with LlamaGen [6], we adopt standard transformer configs that jointly scale L , d and the number of attention heads. Specifically, we establish four configs: LASAD-B, LASAD-L, LASAD-XL and LASAD-XXL. These configurations span a broad range of model sizes and parameter distributions, ranging from 111M to 1.4B parameters, enabling us to evaluate the impact of scaling. Detailed information about these configurations is provided in Tab. 1.

4.3. Ordinary Linear Attention Adaptation

We first conduct experiments to answer the question posed in Sec. 1: “Can linear attention be effectively applied to autoregressive image generation models without compromising performance?”.

In Table 2, we present the performance of various linear attention variants on autoregressive image generation tasks. We first examine two baseline experiments: “LinearAttn” and “Hybrid-Linear”. The former implements ba-



Figure 2. **Autoregressive Image Generation with LASADGen.** We show the samples from our class-conditional LASADGen-XL model trained on ImageNet at 256×256 resolution.

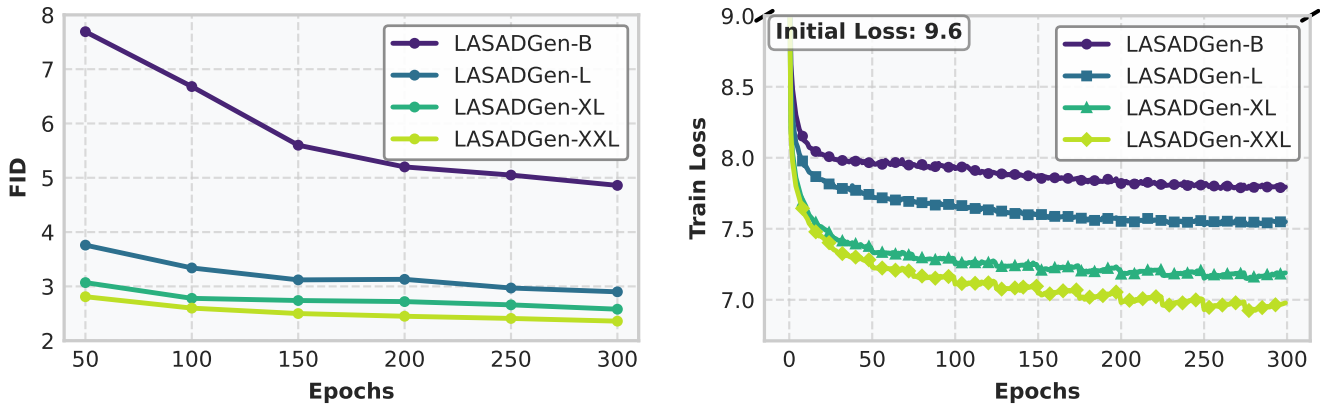


Figure 3. **Scaling properties of LASADGen.** **Left:** FID scores and **Right:** Training loss vs. model size.

asic linear attention by directly substituting kernel functions for the softmax operation [20], while the latter employs a hybrid architecture [18] that intersperses only one standard attention layer among linear attention layers. Our results indicate that basic linear attention fails entirely to adapt to this task. The hybrid attention model demonstrates substantial performance improvements over basic linear attention by effectively combining softmax attention’s superior long-range dependency modeling capabilities with linear atten-

tion’s computational efficiency. However, despite these advantages, hybrid model still underperforms compared to our proposed LASAD approach. We further investigate two decay-based linear attention mechanisms: TNL [17] and GLA [22]. Our analysis reveals that these models demonstrate notable performance deficiencies when compared to our proposed LASAD approach. These experimental results indicate that advanced linear attention architectures incorporating decay mechanisms still fail to achieve optimal ef-

Table 2. **Quantitative comparisons** of different architectures for autoregressive image generation. “LinearAttn” denotes the original linear attention augmented with RoPE [56]. “Hybrid-Linear” refers to the hybrid architecture that integrates one softmax attention layer within the LinearAttn framework. “SoftmaxAttn” represents the conventional softmax-based attention mechanism. TNL and GLA represent two decay-based methods respectively.

Size	Model	FID↓	IS↑	Precision↑	Recall↑
B	LinearAttn [20]	50.86	19.27	0.45	0.40
	SoftmaxAttn	5.46	193.61	0.83	0.45
	Hybrid-Linear	6.36	163.65	0.81	0.46
	TNL [17]	6.75	161.92	0.80	0.46
	GLA [22]	6.45	163.21	0.80	0.47
	LASADGen	4.86	194.91	0.82	0.48
L	LinearAttn [20]	37.50	28.99	0.53	0.43
	SoftmaxAttn	3.80	248.28	0.83	0.51
	Hybrid-Linear	3.64	224.67	0.81	0.52
	TNL [17]	3.61	228.51	0.81	0.51
	GLA [22]	3.58	234.21	0.81	0.51
	LASADGen	2.90	255.61	0.82	0.55

ficacy in autoregressive image generation tasks, although they have been validated on language models.

4.4. Performance Comparison

Quantitative Comparison. We compare the performance of our proposed LASADGen with prior image generation methods, as presented in Tab. 3. To demonstrate the generality of our model, we evaluate results across four different behavior. Our method consistently achieves significantly superior image generation quality compared to state-of-the-art autoregressive methods, highlighting its robustness and effectiveness. Notably, LASADGen outperforms LlamaGen across all model sizes tested. Moreover, our model trained at 256×256 resolution surpasses the performance of LlamaGen at 384×384 resolution.

Furthermore, for a more complete comparison with LlamaGen, which does not report results at 300 epochs for their XL and XXL models (trained at 256×256 resolution), we present additional results for our LASADGen at 50 epochs using the XL and XXL models. As indicated by the results marked with \dagger in Tab. 3, LASADGen demonstrates superior performance even under shorter training epochs, further validating its effectiveness. This can also be demonstrated in Fig. 4, which shows that our LASADGen exhibits strong convergence ability in the first 50 epochs.

Visualization. As shown in Fig. 2, we visualize some sample images randomly generated by our LASADGen. We can observe that LASADGen is capable of generating high-quality samples with both high fidelity and diversity. The generated images exhibit remarkable structural coherence and fine-grained details, particularly in complex textures

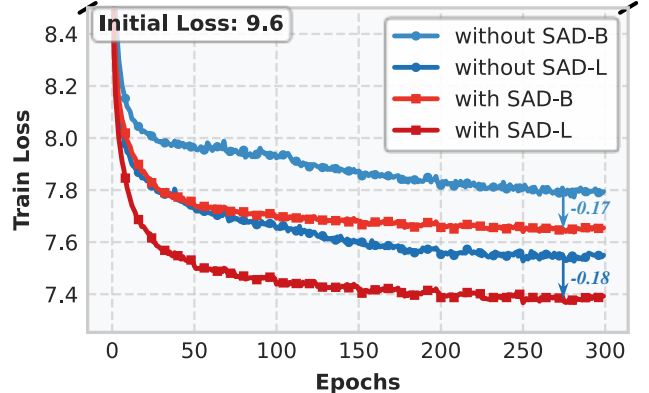


Figure 4. **Training loss comparison between the model with or without the proposed Spatial-Aware Decay.** We visualize the training process of the two groups of models in Tab. 4. The blue curve is used to represent the model without using SAD, and the red curve is used to represent the model using SAD.

and object boundaries. These visualizations substantiate the effectiveness of our proposed architectural improvements by the LASADGen.

Efficiency Analysis. Fig. 5 illustrates a comparative analysis of inference speed and performance between our proposed LASADGen and several other representative methodologies across various model sizes. Among these comparisons, LlamaGen serves as our baseline methodology, while DiT [4] represents a typical architecture based on the diffusion model [11] framework. The results demonstrate that at equivalent model sizes, our approach consistently achieves superior inference speeds. This advantage is due to the linear computational complexity of our model architecture.

Scaling Model Scales. We investigate the scaling behavior of LASADGen. As shown in Fig. 3, we show the training loss and FID score based on models of different sizes on different training iterations. It can be observed that LASADGen demonstrates good scalability, with lower training loss and better FID scores as the model size increases. This is because we did not modify the structure of the AR model itself, preserving the integrity of the AR framework, and therefore inheriting the scalability of AR methods.

4.5. Ablations of the Spatial-Aware Decay

To validate the effectiveness of our proposed Spatial-Aware Decay (SAD) mechanism, we conduct ablation studies on both base (B) and large (L) model variants. As shown in Fig. 4, incorporating SAD consistently leads to improved training dynamics across model scales. Both LASADGen-B and LASADGen-L variants demonstrate more efficient optimization, achieving lower training loss values throughout the training process. Particularly noteworthy is the significant gap between models with and without SAD after convergence. This improvement in optimization efficiency directly translates to enhanced generation quality, as evi-

Table 3. **Class-conditional generation on 256×256 ImageNet.** * specifies the generated images are 384×384 and are resized to 256×256 for evaluation. “-re” denotes rejection sampling is used. † indicates the performance after only 50 epochs of training. The evaluation protocol and implementation are the same with ADM.

Model	#Para.	FID↓	IS↑	Precision↑	Recall↑
VQGAN [57]	227M	18.65	80.4	0.78	0.26
VQGAN [57]	1.4B	15.78	74.3	—	—
VQGAN-re [57]	1.4B	5.20	280.3	—	—
ViT-VQGAN [58]	1.7B	4.17	175.1	—	—
ViT-VQGAN-re [58]	1.7B	3.04	227.4	—	—
RQTran. [59]	3.8B	7.55	134.0	—	—
RQTran.-re [59]	3.8B	3.80	323.7	—	—
<hr/>					
LlamaGen-B* [6]	111M	6.43	157.17	0.81	0.46
LlamaGen-L* [6]	343M	3.07	256.06	0.83	0.52
LlamaGen-XL* [6]	775M	2.62	244.08	0.80	0.57
LlamaGen-XXL* [6]	1.4B	2.34	253.90	0.80	0.59
LlamaGen-B [6]	111M	5.46	193.61	0.83	0.45
LlamaGen-L [6]	343M	3.80	248.28	0.83	0.51
LlamaGen-XL† [6]	775M	3.39	227.08	0.81	0.54
LlamaGen-XXL† [6]	1.4B	3.09	253.61	0.83	0.53
<hr/>					
LASADGen-B	112M	4.86	194.91	0.82	0.48
LASADGen-L	346M	2.90	255.61	0.82	0.55
LASADGen-XL	774M	2.58	282.73	0.82	0.56
LASADGen-XXL	1.4B	2.36	283.2	0.82	0.57
LASADGen-XL†	774M	3.07	269.35	0.83	0.54
LASADGen-XXL†	1.4B	2.81	270.42	0.83	0.55

Table 4. **Quantitative comparisons** of the model with or without the proposed SAD.

Size	Model	SAD	FID↓	IS↑	Precision↑	Recall↑
B	GLA [22]	✗	6.45	163.21	0.80	0.47
	GLA [22]	✓	5.84	173.00	0.80	0.48
	LASADGen	✗	7.42	151.02	0.78	0.47
	LASADGen	✓	4.86	194.91	0.82	0.48
L	LASADGen	✗	3.73	231.88	0.81	0.51
	LASADGen	✓	2.90	255.61	0.82	0.55

denced by the quantitative metrics Tab. 4. We observe substantial improvements in FID scores for both model sizes, with similar gains in Inception Score. The precision and recall metrics also show consistent improvements, indicating that SAD enhances both the fidelity and diversity of generated samples. Furthermore, we apply our proposed SAD to GLA-B [22] and conduct experiments. The experimental results show that SAD can also produce performance gains for GLA. These results confirm that our proposed Spatial-Aware Decay mechanism effectively addresses the limitations of the baseline linear attention model, leading to more coherent and visually appealing image generation.

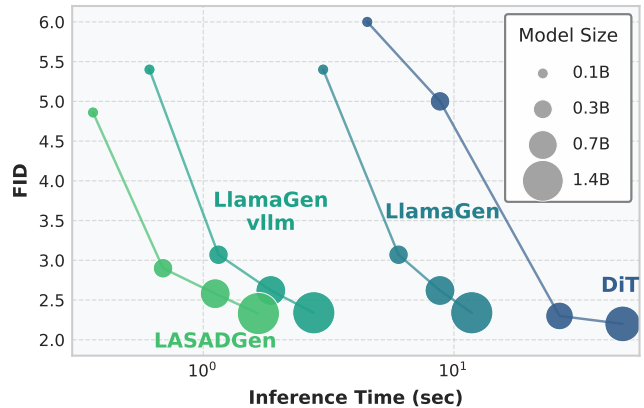


Figure 5. **Comparative Analysis of inference Speed.** All tests are performed on 8 NVIDIA H800 GPUs.

5. Conclusion

In this paper, we proposed LASADGen, a novel autoregressive image generation model incorporating Linear Attention with Spatial-Aware Decay (LASAD). Our method effectively preserves 2D spatial relationships within flattened sequences, overcoming critical limitations of existing linear attention mechanisms originally designed for 1D sequential data. Experimental results on ImageNet demonstrate

that LASADGen achieves state-of-the-art image generation quality with significantly reduced computational complexity. Future research directions include adapting LASAD for variable-resolution generation and expanding its application to larger-scale tasks, such as text-to-image generation or video generation. This work opens promising directions for efficient autoregressive modeling of spatial contexts in visual data and highlights the potential of spatial-aware attention.

6. Acknowledgments

This research was supported in part by National Natural Science Foundation of China (62271410, 12150007) and by the Fundamental Research Funds for the Central Universities. Yuxin Mao is sponsored by the Innovation Foundation for Doctoral Dissertation of Northwestern Polytechnical University (CX2024014).

References

- [1] Prafulla Dhariwal and Alexander Nichol. Diffusion models beat gans on image synthesis. *Conference on Neural Information Processing Systems (NeurIPS)*, 34:8780–8794, 2021. [1](#)
- [2] Jonathan Ho, Chitwan Saharia, William Chan, David J Fleet, Mohammad Norouzi, and Tim Salimans. Cascaded diffusion models for high fidelity image generation. *Journal of Machine Learning Research (JMLR)*, 23(1):2249–2281, 2022.
- [3] Robin Rombach, Andreas Blattmann, Dominik Lorenz, Patrick Esser, and Björn Ommer. High-resolution image synthesis with latent diffusion models. In *Conference on Computer Vision and Pattern Recognition (CVPR)*, pages 10684–10695, 2022. [2](#)
- [4] William Peebles and Saining Xie. Scalable diffusion models with transformers. In *Conference on Computer Vision and Pattern Recognition (CVPR)*, pages 4195–4205, 2023. [7](#)
- [5] Yuxin Mao, Xuyang Shen, Jing Zhang, Zhen Qin, Jinxing Zhou, Mochu Xiang, Yiran Zhong, and Yuchao Dai. Tavgbench: Benchmarking text to audible-video generation. In *ACM Multimedia Conference (ACM MM)*, pages 6607–6616, 2024.
- [6] Peize Sun, Yi Jiang, Shoufa Chen, Shilong Zhang, Bingyu Peng, Ping Luo, and Zehuan Yuan. Autoregressive model beats diffusion: Llama for scalable image generation. *arXiv preprint arXiv:2406.06525*, 2024. [2](#), [3](#), [5](#), [8](#)
- [7] Zhen Qin, Yuxin Mao, Xuyang Shen, Dong Li, Jing Zhang, Yuchao Dai, and Yiran Zhong. You only scan once: Efficient multi-dimension sequential modeling with lightnet. *arXiv preprint arXiv:2405.21022*, 2024. [1](#)
- [8] Andrew Brock, Jeff Donahue, and Karen Simonyan. Large scale gan training for high fidelity natural image synthesis. *arXiv preprint arXiv:1809.11096*, 2018. [1](#)
- [9] Minguk Kang, Jun-Yan Zhu, Richard Zhang, Jaesik Park, Eli Shechtman, Sylvain Paris, and Taesung Park. Scaling up gans for text-to-image synthesis. In *Conference on Computer Vision and Pattern Recognition (CVPR)*, pages 10124–10134, 2023.
- [10] Axel Sauer, Katja Schwarz, and Andreas Geiger. Stylegan-xl: Scaling stylegan to large diverse datasets. In *ACM SIGGRAPH*, pages 1–10, 2022. [1](#)
- [11] Jonathan Ho, Ajay Jain, and Pieter Abbeel. Denoising diffusion probabilistic models. *Conference on Neural Information Processing Systems (NeurIPS)*, 33:6840–6851, 2020. [1](#), [7](#)
- [12] Hugo Touvron, Thibaut Lavril, Gautier Izacard, Xavier Martinet, Marie-Anne Lachaux, Timothée Lacroix, Baptiste Rozière, Naman Goyal, Eric Hambro, Faisal Azhar, et al. Llama: Open and efficient foundation language models. *arXiv preprint arXiv:2302.13971*, 2023. [1](#), [2](#)
- [13] Alec Radford, Karthik Narasimhan, Tim Salimans, Ilya Sutskever, et al. Improving language understanding by generative pre-training. 2018. [2](#)
- [14] Aixin Liu, Bei Feng, Bing Xue, Bingxuan Wang, Bochao Wu, Chengda Lu, Chenggang Zhao, Chengqi Deng, Chenyu Zhang, Chong Ruan, et al. Deepseek-v3 technical report. *arXiv preprint arXiv:2412.19437*, 2024. [1](#)
- [15] Ashish Vaswani, Noam Shazeer, Niki Parmar, Jakob Uszkoreit, Llion Jones, Aidan N Gomez, Łukasz Kaiser, and Illia Polosukhin. Attention is all you need. *Conference on Neural Information Processing Systems (NeurIPS)*, 30, 2017. [1](#), [3](#)
- [16] Xuyang Shen, Dong Li, Ruitao Leng, Zhen Qin, Weigao Sun, and Yiran Zhong. Scaling laws for linear complexity language models. *arXiv preprint arXiv:2406.16690*, 2024. [1](#)
- [17] Zhen Qin, Weigao Sun, Dong Li, Xuyang Shen, Weixuan Sun, and Yiran Zhong. Various lengths, constant speed: Efficient language modeling with lightning attention. In *International Conference on Machine Learning (ICML)*, 2024. [1](#), [2](#), [6](#), [7](#)
- [18] Aonian Li, Bangwei Gong, Bo Yang, Boji Shan, Chang Liu, Cheng Zhu, Chunhao Zhang, Congchao Guo, Da Chen, Dong Li, et al. Minimax-01: Scaling foundation models with lightning attention. *arXiv preprint arXiv:2501.08313*, 2025. [1](#), [6](#)
- [19] Opher Lieber, Barak Lenz, Hofit Bata, Gal Cohen, Jhonathan Osin, Itay Dalmedigos, Erez Safahi, Shaked Meir, Yonatan Belinkov, Shai Shalev-Shwartz, et al. Jamba: A hybrid transformer-mamba language model. *arXiv preprint arXiv:2403.19887*, 2024. [1](#)
- [20] Angelos Katharopoulos, Apoorv Vyas, Nikolaos Pappas, and François Fleuret. Transformers are rnns: Fast autoregressive transformers with linear attention. In *International Conference on Machine Learning (ICML)*, pages 5156–5165. PMLR, 2020. [1](#), [2](#), [3](#), [4](#), [6](#), [7](#)
- [21] Zhen Qin, Weixuan Sun, Hui Deng, Dongxu Li, Yunshen Wei, Baohong Lv, Junjie Yan, Lingpeng Kong, and Yiran Zhong. cosformer: Rethinking softmax in attention. In *International Conference on Learning Representations (ICLR)*, 2022. [1](#), [2](#), [3](#)
- [22] Songlin Yang, Bailin Wang, Yikang Shen, Rameswar Panda, and Yoon Kim. Gated linear attention transformers with hardware-efficient training. *arXiv preprint arXiv:2312.06635*, 2023. [1](#), [2](#), [4](#), [6](#), [7](#), [8](#)
- [23] Yutao Sun, Li Dong, Shaohan Huang, Shuming Ma, Yuqing Xia, Jilong Xue, Jianyong Wang, and Furu Wei. Retentive

- network: A successor to transformer for large language models. *arXiv preprint arXiv:2307.08621*, 2023. 2, 4
- [24] Zhen Qin, Songlin Yang, and Yiran Zhong. Hierarchically gated recurrent neural network for sequence modeling. *Conference on Neural Information Processing Systems (NeurIPS)*, 36, 2024. 2, 4
- [25] Zhen Qin, Songlin Yang, Weixuan Sun, Xuyang Shen, Dong Li, Weigao Sun, and Yiran Zhong. Hgrn2: Gated linear rnns with state expansion. *arXiv preprint arXiv:2404.07904*, 2024. 2, 4
- [26] Aili Chen, Aonian Li, Bangwei Gong, Binyang Jiang, Bo Fei, Bo Yang, Boji Shan, Changqing Yu, Chao Wang, Cheng Zhu, et al. Minimax-m1: Scaling test-time compute efficiently with lightning attention. *arXiv preprint arXiv:2506.13585*, 2025. 1
- [27] Jia Deng, Wei Dong, Richard Socher, Li-Jia Li, Kai Li, and Li Fei-Fei. Imagenet: A large-scale hierarchical image database. In *Conference on Computer Vision and Pattern Recognition (CVPR)*, pages 248–255. Ieee, 2009. 2, 5
- [28] Huiwen Chang, Han Zhang, Lu Jiang, Ce Liu, and William T Freeman. Maskgit: Masked generative image transformer. In *Conference on Computer Vision and Pattern Recognition (CVPR)*, pages 11315–11325, 2022. 2
- [29] Tianhong Li, Huiwen Chang, Shlok Mishra, Han Zhang, Dina Katabi, and Dilip Krishnan. Mage: Masked generative encoder to unify representation learning and image synthesis. In *Conference on Computer Vision and Pattern Recognition (CVPR)*, pages 2142–2152, 2023.
- [30] Tianhong Li, Yonglong Tian, He Li, Mingyang Deng, and Kaiming He. Autoregressive image generation without vector quantization. *Conference on Neural Information Processing Systems (NeurIPS)*, 37:56424–56445, 2025.
- [31] Lijun Yu, Yong Cheng, Kihyuk Sohn, José Lezama, Han Zhang, Huiwen Chang, Alexander G Hauptmann, Ming-Hsuan Yang, Yuan Hao, Irfan Essa, et al. Magvit: Masked generative video transformer. In *Conference on Computer Vision and Pattern Recognition (CVPR)*, pages 10459–10469, 2023. 2
- [32] Jacob Devlin, Ming-Wei Chang, Kenton Lee, and Kristina Toutanova. Bert: Pre-training of deep bidirectional transformers for language understanding. In *Association for Computational Linguistics (ACL)*, pages 4171–4186, 2019. 2
- [33] Patrick Esser, Robin Rombach, and Bjorn Ommer. Taming transformers for high-resolution image synthesis. In *Conference on Computer Vision and Pattern Recognition (CVPR)*, pages 12873–12883, 2021. 2
- [34] Jiahui Yu, Xin Li, Jing Yu Koh, Han Zhang, Ruoming Pang, James Qin, Alexander Ku, Yuanzhong Xu, Jason Baldridge, and Yonghui Wu. Vector-quantized image modeling with improved vqgan. *arXiv preprint arXiv:2110.04627*, 2021. 2
- [35] Diederik P Kingma and Max Welling. Auto-encoding variational bayes. *arXiv preprint arXiv:1312.6114*, 2013. 2
- [36] Aaron Van Den Oord, Oriol Vinyals, et al. Neural discrete representation learning. *Conference on Neural Information Processing Systems (NeurIPS)*, 30, 2017. 2
- [37] Keyu Tian, Yi Jiang, Zehuan Yuan, Bingyue Peng, and Liwei Wang. Visual autoregressive modeling: Scalable image generation via next-scale prediction. *arXiv preprint arXiv:2404.02905*, 2024. 2
- [38] Yuqing Wang, Shuhuai Ren, Zhijie Lin, Yujin Han, Haoyuan Guo, Zhenheng Yang, Difan Zou, Jiashi Feng, and Xihui Liu. Parallelized autoregressive visual generation. *arXiv preprint arXiv:2412.15119*, 2024. 2
- [39] Yatian Pang, Peng Jin, Shuo Yang, Bin Lin, Bin Zhu, Zhenyu Tang, Liuhan Chen, Francis EH Tay, Ser-Nam Lim, Harry Yang, et al. Next patch prediction for autoregressive visual generation. *arXiv preprint arXiv:2412.15321*, 2024.
- [40] Yefei He, Feng Chen, Yuanyu He, Shaoxuan He, Hong Zhou, Kaipeng Zhang, and Bohan Zhuang. Zipar: Accelerating autoregressive image generation through spatial locality. *arXiv preprint arXiv:2412.04062*, 2024. 2
- [41] Xiang Li, Kai Qiu, Hao Chen, Jason Kuen, Jiuxiang Gu, Bhiksha Raj, and Zhe Lin. Imagefolder: Autoregressive image generation with folded tokens. *arXiv preprint arXiv:2410.01756*, 2024. 2
- [42] Haopeng Li, Jinyue Yang, Kexin Wang, Xuerui Qiu, Yuhong Chou, Xin Li, and Guoqi Li. Scalable autoregressive image generation with mamba. *arXiv preprint arXiv:2408.12245*, 2024. 2
- [43] Xuanton Liu, Shaozhe Hao, Xianbiao Qi, Tianyang Hu, Jun Wang, Rong Xiao, and Yuan Yao. Elucidating the design space of language models for image generation. *arXiv preprint arXiv:2410.16257*, 2024. 2
- [44] Hao Peng, Nikolaos Pappas, Dani Yogatama, Roy Schwartz, Noah Smith, and Lingpeng Kong. Random feature attention. In *International Conference on Learning Representations (ICLR)*, 2020. 2
- [45] Krzysztof Marcin Choromanski, Valerii Likhoshesterov, David Dohan, Xingyou Song, Andreea Gane, Tamas Sarrlos, Peter Hawkins, Jared Quincy Davis, Afroz Mohiuddin, Lukasz Kaiser, et al. Rethinking attention with performers. In *International Conference on Learning Representations (ICLR)*, 2020. 2, 3
- [46] Zhen Qin, Xiaodong Han, Weixuan Sun, Dongxu Li, Lingpeng Kong, Nick Barnes, and Yiran Zhong. The devil in linear transformer. In *Conference on Empirical Methods in Natural Language Processing (EMNLP)*, pages 7025–7041, 2022. 3
- [47] Zhen Qin, Dong Li, Weigao Sun, Weixuan Sun, Xuyang Shen, Xiaodong Han, Yunshen Wei, Baohong Lv, Xiao Luo, Yu Qiao, and Yiran Zhong. Transnormerllm: A faster and better large language model with improved transnormer. *arXiv preprint arXiv:2307.14995*, 2023. 4
- [48] Albert Gua, Caglar Gulcehre, Tom le Paine, Razvan Pascanu, and Matt Hoffman. Improving the gating mechanism of recurrent neural networks, 2020. 4
- [49] Albert Gu and Tri Dao. Mamba: Linear-time sequence modeling with selective state spaces. *arXiv preprint arXiv:2312.00752*, 2023. 4
- [50] Martin Heusel, Hubert Ramsauer, Thomas Unterthiner, Bernhard Nessler, and Sepp Hochreiter. Gans trained by a two time-scale update rule converge to a local nash equilibrium. *Conference on Neural Information Processing Systems (NeurIPS)*, 30, 2017. 5

- [51] Tim Salimans, Ian Goodfellow, Wojciech Zaremba, Vicki Cheung, Alec Radford, and Xi Chen. Improved techniques for training gans. *Conference on Neural Information Processing Systems (NeurIPS)*, 29, 2016. 5
- [52] Tuomas Kynkäänniemi, Tero Karras, Samuli Laine, Jaakko Lehtinen, and Timo Aila. Improved precision and recall metric for assessing generative models. *Conference on Neural Information Processing Systems (NeurIPS)*, 32, 2019. 5
- [53] Prafulla Dhariwal and Alexander Nichol. Diffusion models beat gans on image synthesis. *Conference on Neural Information Processing Systems (NeurIPS)*, 34:8780–8794, 2021. 5
- [54] Jonathan Ho and Tim Salimans. Classifier-free diffusion guidance. *arXiv preprint arXiv:2207.12598*, 2022. 5
- [55] Songlin Yang and Yu Zhang. Fla: A triton-based library for hardware-efficient implementations of linear attention mechanism, January 2024. 5
- [56] Jianlin Su, Murtadha Ahmed, Yu Lu, Shengfeng Pan, Wen Bo, and Yunfeng Liu. Roformer: Enhanced transformer with rotary position embedding. *Neurocomputing*, 568:127063, 2024. 7
- [57] Patrick Esser, Robin Rombach, and Björn Ommer. Taming transformers for high-resolution image synthesis. In *Conference on Computer Vision and Pattern Recognition (CVPR)*, pages 12873–12883, 2021. 8
- [58] Jiahui Yu, Xin Li, Jing Yu Koh, Han Zhang, Ruoming Pang, James Qin, Alexander Ku, Yuanzhong Xu, Jason Baldridge, and Yonghui Wu. Vector-quantized image modeling with improved VQGAN. In *International Conference on Learning Representations (ICLR)*, 2022. 8
- [59] Doyup Lee, Chiheon Kim, Saehoon Kim, Minsu Cho, and Wook-Shin Han. Autoregressive image generation using residual quantization. In *Conference on Computer Vision and Pattern Recognition (CVPR)*, pages 11513–11522, 2022. 8